Inorg. Chem. **2008**, *47*, 7048−7058

Trichromophoric Systems from Square-Planar Pt-Ethynylbipyridine and Octahedral Ru- and Os-Bipyridine Centers: Syntheses, Structures, Electrochemical Behavior, and Bipartition of Energy Transfer

Barbara Ventura,*,† Andrea Barbieri,† Francesco Barigelletti,† Julie Batcha Seneclauze,‡ Pascal Retailleau,§ and Raymond Ziessel*,‡

Istituto per la Sintesi Organica e la Fotoreattività, Consiglio Nazionale delle Ricerche (ISOF-CNR), Via P. Gobetti 101, 40129 Bologna, Italy, Laboratoire de Chimie Moléculaire, Ecole de Chimie, Polymères, Matériaux (ECPM), Université Louis Pasteur (ULP), 25 rue Becquerel, 67087 Strasbourg Cedex 02, France, and Laboratoire de Cristallochimie, ICSN - CNRS, Bât 27 - 1 avenue de la Terrasse, 91198 Gif-sur-Yvette, Cedex, France

Received April 28, 2008

The synthetic approach, electrochemical behavior, and optical absorption and emission properties are reported of the Pt-bipyridine-acetylide/Ru-bipyridine complex $[(dbbpy)Pt\{(ebpy)Ru(bpy)_2\}_2]^{4+}$, $PtRu_2$, the Pt-bipyridine-acetylide/Os-bipyridine analogue, $PtOs_2$, and the Pt/Ru/Os complex $[(dbbpy)Pt(ebpy)_2Ru(bpy)_2Os(bpy)_2]^{4+}$, PtRuOs; ebpy is 5-ethynylbpy, dbbpy is 4,4′-ditertiobutylbpy, and bpy is 2,2′-bipyridine. These triads are investigated in acetonitrile solvent by comparing their electrochemical and spectroscopic properties with those of the mononuclear species $[(dbbpy)Pt(ebpy)_2]$, Pt, $[Ru(ebpy)(bpy)_2]^{2+}$, Ru, and $[Os(ebpy)(bpy)_2]^{2+}$, Os. Results of X-ray analysis of Pt are reported, which show the planar arrangement of this unit that features two free bpy sites. The absorption spectra of the triads and the mononuclear species show that light at 452 or 376 nm can be employed to observe luminescence spectra of these complexes; for the observation of emission lifetimes, nanoled sources at 465 and 373 nm are employed. With $\lambda_{exc} = 452$ (and 465) nm, one selectively produces Ru → bpy/ebpy CT (RuLCT) or Os → bpy/ebpy CT states (OsLCT); MLCT is a metal-to-ligand charge-transfer. With $\lambda_{exc} = 376$ (and 373) nm, one populates Pt → dbbpy CT and intraligand charge transfer (ILCT, involving the ebpy fragment) levels, in addition to Ru(II)- or Os(II)-centered excited states, in aliquots that are estimated from comparison of the absorption features of the components. Upon excitation with light at 376 (and 373) nm, the optical studies of $PtRu_2$, $PtOs_2$, and PtRuOs reveal full quenching of the Pt-based emission and occurrence of efficient photoinduced energy transfer, leading to exclusive MLCT emission from the ruthenium and osmium centers. In particular, PtRuOs is found to exhibit a Ru- and Os-based dual luminescence, whose intensities ratio is consistent with a Pt → Os intramolecular energy transfer step being 3−6 times faster than the Pt → Ru one.

Introduction

Square planar platinum(II) diimine complexes containing acetylide ligands, $[Pt(N^N)(C{\equiv}C{-}R)_2]$, are a family of neutral and strongly luminescent compounds;[1–7] (N^N) is typically a substituted bpy (2,2′-bipyridine) or phen (1,10-phenanthroline) ligand; R is a substituted aryl group. Light absorption in these complexes yields ^{1}MLCT (of Pt(d) → (N^N)π^* nature), ^{1}MC (dd), and ^{1}LC ($\pi\pi^*$) states, and owing to the high spin−orbit coupling constant of the Pt center

* To whom correspondence should be addressed. E-mail: bventura@isof.cnr.it (B.V.), ziessel@chimie.u-strasbg.fr (R.Z.).
† Consiglio Nazionale delle Ricerche (ISOF-CNR).
‡ Université Louis Pasteur (ULP).
§ ICSN - CNRS.

(1) Chan, C. W.; Cheng, L. K.; Che, C. M. *Coord. Chem. Rev.* **1994**, *132*, 87–97.
(2) Williams, J. A. G. *Top. Curr. Chem.* **2007**, *281*, 205–268.
(3) Hissler, M.; Connick, W. B.; Geiger, D. K.; McGarrah, J. E.; Lipa, D.; Lachicotte, R. J.; Eisenberg, R. *Inorg. Chem.* **2000**, *39*, 447–457.
(4) Whittle, C. E.; Weinstein, J. A.; George, M. W.; Schanze, K. S. *Inorg. Chem.* **2001**, *40*, 4053–4062.
(5) Wadas, T. J.; Lachicotte, R. J.; Eisenberg, R. *Inorg. Chem.* **2003**, *42*, 3772–3778.
(6) Castellano, F. N.; Pomestchenko, I. E.; Shikhova, E.; Hua, F.; Muro, M. L.; Rajapakse, N. *Coord. Chem. Rev.* **2006**, *250*, 1819–1828.
(7) Pomestchenko, I. E.; Castellano, F. N. *J. Phys. Chem. A* **2004**, *108*, 3485–3492.

10.1021/ic800768v CCC: $40.75
Published on Web 06/27/2008

Chart 1. Molecular Structures of the Pt Precursor, Mononuclear Ru, and Os Complexes, and Di- and Trinuclear Pt/Ru Complexes

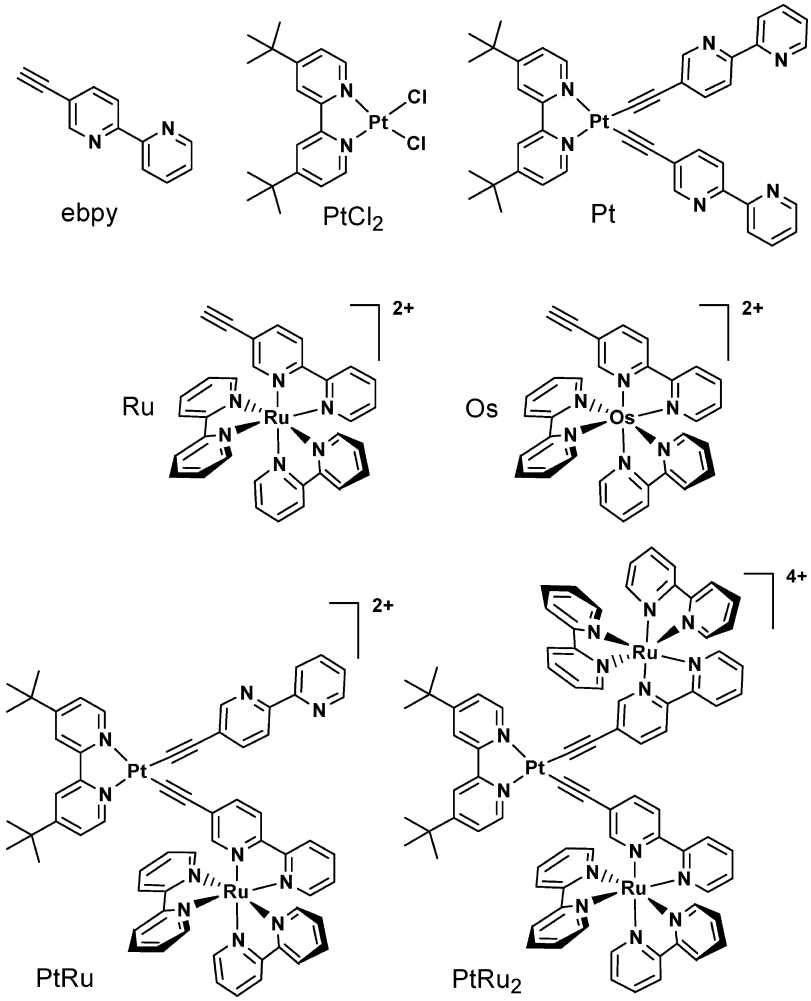

($\zeta = 4{,}481\ cm^{-1}$),[8] the observed emission exhibits a triplet character. The strong field acetylide ligands raise the energy of the dd states and a predominant ^{3}MLCT emission is detected, sometimes with relevant contributions from $^3\pi\pi^*$ levels.[7] In degassed solvent and dilute conditions to avoid excimer formation, for these Pt ← (N^N) CT emitters the luminescence quantum yield, ϕ_{em}, is frequently larger than 0.1 with a wavelength maximum λ_{em} typically around 580 nm and a lifetime τ_{em} on the order of 1 μs.[2]

In multichromophoric assemblies containing the Pt−diimine−acetylide center, both photoinduced charge separation[3,9,10] and energy transfer[11−13] have been investigated. For instance, within [Pt(N^N)(C≡CR)$_2$] systems where R is pyrene or perylenediimide (PDI), excitation into the lowest energy ^{1}MLCT absorption band of the complex yields luminescence properties of intrapyrene or intra-PDI $^3\pi\pi^*$ character, indicative of efficient MLCT → $\pi\pi^*$ sensitization.[11,14,15] With regard to multimetallic species, in systems comprising Pt−diimine−acetylide complexes and lanthanide−diketonate fragments, upon excitation into the ^{1}MLCT band, sensitized near-infrared emission is observed from the Ln(III) center.[13,16]

In a preliminary communication, we reported on the use of a 5-ethynylbpy precursor, ebpy, to yield the complexes [(dbbpy)Pt(ebpy)$_2$], Pt, and [Ru(ebpy)(bpy)$_2$]$^{2+}$, Ru, the former containing two free bpy sites, see Chart 1; dbbpy is 4,4′-ditertiobutylbpy.[17] This allowed the study of the optical properties of the [(dbbpy)Pt(ebpy)$_2$Ru(bpy)$_2$]$^{2+}$ dyad, PtRu, and the [(dbbpy)Pt{(ebpy)Ru(bpy)$_2$}$_2$]$^{4+}$ triad, PtRu$_2$ Chart 1, in which Pt(II) planar and Ru(II) octahedral metal centers were held together for the first time. For the mixed-metal PtRu and PtRu$_2$ complexes, comparison with the absorption

(8) Montalti, M.; Credi, A.; Prodi, L.; Gandolfi, M. T. *Handbook of Photochemistry, 3rd Edition*; CRC Press, Taylor & Francis: Boca Raton, 2006; p 617.
(9) McGarrah, J. E.; Eisenberg, R. *Inorg. Chem.* **2003**, *42*, 4355–4365.
(10) Chakraborty, S.; Wadas, T. J.; Hester, H.; Schmehl, R.; Eisenberg, R. *Inorg. Chem.* **2005**, *44*, 6865–6878.
(11) Danilov, E. O.; Pomestchenko, I. E.; Kinayyigit, S.; Gentili, P. L.; Hissler, M.; Ziessel, R.; Castellano, F. N. *J. Phys. Chem. A* **2005**, *109*, 2465–2471.
(12) Lam, S. C. F.; Yam, V. W. W.; Wong, K. M. C.; Cheng, E. C. C.; Zhu, N. Y. *Organometallics* **2005**, *24*, 4298–4305.
(13) Ronson, T. K.; Lazarides, T.; Adams, H.; Pope, S. J. A.; Sykes, D.; Faulkner, S.; Coles, S. J.; Hursthouse, M. B.; Clegg, W.; Harrington, R. W.; Ward, M. D. *Chem.—Eur. J.* **2006**, *12*, 9299–9313.
(14) Pomestchenko, I. E.; Luman, C. R.; Hissler, M.; Ziessel, R.; Castellano, F. N. *Inorg. Chem.* **2003**, *42*, 1394–1396.
(15) Rachford, A. A.; Goeb, S.; Castellano, F. N. *J. Am. Chem. Soc.* **2008**, *130*, 2766.
(16) Ziessel, R.; Diring, S.; Kadjane, P.; Charbonniere, L.; Retailleau, P.; Philouze, C. *Chem.—Asian J.* **2007**, *2*, 975–982.
(17) Ziessel, R.; Seneclauze, J. B.; Ventura, B.; Barbieri, A.; Barigelletti, F. *Dalton Trans.* **2008**, 1686–1688.

Chart 2. Molecular Structures of the Trinuclear Complexes Containing the Os-Based Unit

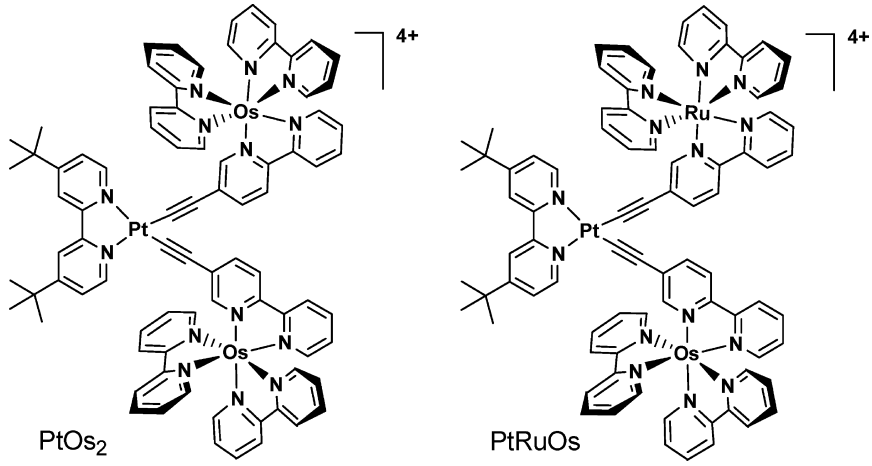

properties of the mononuclear species Pt and Ru, allowed us to label two absorption bands in the visible region. The one peaking at lower energy (λ_{max} = 452 and 454 nm, ε = 13 700 and 24 100 M^{-1} cm^{-1}, for PtRu and $PtRu_2$, respectively) was attributed to Ru → bpy/ebpy CT nature (RuLCT).[18] The higher energy band (λ_{max} = 376 and 366 nm, ε = 35 600 and 52 600 M^{-1} cm^{-1}, for PtRu and $PtRu_2$, respectively) was due to transitions to ^{1}Pt → dbbpy CT and ^{1}ILCT states (the latter involving the C≡C−bpy fragment), in addition to ^{1}Ru-based ones.[17] For both PtRu and $PtRu_2$, excitation in this high energy band was found to result in exclusive Ru-based emission, as a consequence of effective Pt → Ru and ILCT → Ru energy transfer processes.

Herein, we provide full details on the control synthesis of mixed-metal Pt-bipyridine-acetylide/Ru-bipyridine complexes, on the characterization of the complexes Pt, Ru, PtRu, and $PtRu_2$, and on the preparation, characterization and optical absorption and emission features of the mononuclear complex $[Os(ebpy)(bpy)_2]^{2+}$, Os, and of the trimetallic complexes $[(dbbpy)Pt\{(ebpy)Os(bpy)_2\}_2]^{4+}$, $PtOs_2$, and $[(dbbpy)Pt(ebpy)_2Ru(bpy)_2Os(bpy)_2]^{4+}$, PtRuOs, Chart 2. For $PtRu_2$, $PtOs_2$, and PtRuOs, upon photoexcitation at 376 nm, the optical studies reveal the occurrence of photoinduced energy transfer from the excited platinum center to both the Ru and Os centers. In particular, for the PtRuOs species the portion of initial excitation localized at the Pt center results in asymmetric Pt → Ru and Pt → Os energy transfer steps leading to sensitization of the Ru and Os units. These energy transfer steps are disentangled and discussed by making use of the optical and electrochemical data of the reference mononuclear complexes presented herein.

Experimental Section

General Methods. 200.1 (^{1}H), 400 (^{1}H), 50.3 (^{13}C), and 100.3 (^{13}C) MHz NMR spectra were recorded at room temperature using the residual proton resonances in deuterated solvents as internal references. Chromatographic purification was conducted using standardized alumina. Thin layer chromatography (TLC) was performed on silica gel plates coated with a fluorescent indicator. All mixtures of solvents are given in v/v ratio.

Materials

4-Ethynyl-2,2′-bipyridine,[19] $[(dbbpy)PtCl_2]$,[20] $[Ru(bpy)]Cl_2 \cdot 2H_2O$,[21] and $[Os(bpy)]Cl_2$[22] were obtained according the respective references.

Preparation of Pt. The preparation began with the dissolution of $[(dbbpy)PtCl_2]$ (0.100 g, 0.187 mmol) in a mixture of DMF (10 mL) and triethylamine (3 mL), followed by the addition of 4-ethynyl-2,2′-bipyridine (0.101 g, 0.561 mmol). The solution was degassed vigorously by bubbling argon through the solution. The addition of CuI (0.002 g, 0.012 mmol) to the slightly yellow solution resulted in the instantaneous color change to deep yellow. After stirring at room temperature for one night, the solvent was removed under reduced pressure and the residue was purified by column chromatography on alumina. The target complex (yellow band) was eluted with a gradient of methanol (0−3%) in dichloromethane as mobile phase. Ultimate recrystallization by slow evaporation of dichloromethane from a dichloromethane/hexane solution afforded a complex of $[(dbbpy)Pt(ebpy)_2]$ Pt (0.120 g, 78%). ^{1}H NMR (400.1 MHz, d^2-dichloromethane): δ 9.64 (d, ^3J = 5.7 Hz, 2H), 8.79 (dd, ^3J = 2.2 Hz, ^4J = 0.7 Hz, 2H), 8.67−8.66 (8 line, m, 2H), 8.44 (td, ^3J = 7.9 Hz, ^4J = 0.7 Hz, 2H), 8.37 (dd, ^3J = 8.1 Hz, ^4J = 0.9 Hz 2H), 8.06 (d, ^3J = 1.8 Hz, 2H), 7.88 (dd, ^3J = 8.1 Hz, ^4J = 2.0 Hz, 2H), 7.83 (dt, ^3J = 7.8 Hz, ^4J = 1.8 Hz 2H), 7.70 (dd, ^3J = 6.1 Hz, ^4J = 1.8 Hz, 2H), 7.32 (dd, ^3J = 4.7 Hz, ^4J = 1.1 Hz, 1H), 7.30 (dd, ^3J = 4.7 Hz, ^4J = 1.1 Hz, 1H), 1.49 (s, 18H). ^{13}C{^{1}H} NMR (100.6 MHz, d^2-dichloromethane) δ 165.1, 157.1, 156.9, 153.0, 152.9, 151.6, 149.9, 140.0, 137.5, 125.8, 125.7, 124.1, 121.5, 120.7, 120.2, 99.4, 94.4, 36.7. FTIR (ATR): ν = 3046 (m), 2965

(18) Juris, A.; Balzani, V.; Barigelletti, F.; Campagna, S.; Belser, P.; von Zelewsky, A. *Coord. Chem. Rev.* **1988**, *84*, 85–277.

(19) Grosshenny, V.; Romero, F. M.; Ziessel, R. *J. Org. Chem.* **1997**, *62*, 1491–1500.

(20) Rendina, L. M.; Vittal, J. J.; Puddephatt, R. J. *Organometallics* **1995**, *14*, 1030–1038.

(21) Sullivan, B. P.; Salmon, D. J.; Meyer, T. J. *Inorg. Chem.* **1978**, *17*, 3334–3341.

(22) Buckingham, D. A.; Dwyer, F. P.; Goodwin, H. A.; Sargeson, A. M. *Aust. J. Chem.* **1964**, *17*, 325–336.

(s), 2110 (s, $\nu_{C'C}$), 1617 (m), 1585 (m), 1568 (m), 1541 (m), 1454 (s), 1432 (m), 1417 (m), 1363 (m), 1251 (m), 1216 (m), 847 (m), 796 (m), 747(m). ESI-MS (CH_3CN) *m/z* 822.3 ($[M+H]^+$. Anal. Calcd for $C_{42}H_{38}N_6Pt$ (M_r = 821.87): C, 61.38; H, 4.66; N, 10.23 Found C, 61.19, H, 4.42, N, 10.02.

Preparation of PtRu. After the dissolution of [(dbbpy)Pt(ebpy)$_2$] (0.042 g, 0.051 mmol) in a mixture of ethanol (20 mL) and dichloromethane (10 mL), 1 equiv of [Ru(bpy)]$Cl_2 \cdot 2H_2O$ (0.026 g, 0.051 mmol) was added. After stirring at reflux overnight, the solvent was removed under reduced pressure. The solid residue was dissolved in a minimum of dimethyformamide (2 mL) and dropwise added into an aqueous solution (2 mL) containing KPF_6 (0.100 g). The complex was recovered by filtration over paper, washed with water (3 × 100 mL), and the red solid dried under high vacuum. Purification was ensured by column chromatography using alumina as solid support and a gradient of methanol (0−1%) in dichloromethane as mobile phase. Ultimate recrystallization by slow evaporation of dichloromethane from a dichloromethane/cyclohexane solution afforded the analytically pure complex [(dbbpy)Pt(ebpy)$_2$Ru(bpy)$_2$]$(PF_6)_2$ PtRu (0.047 g, 67%).^{1}H (400.1 MHz, acetone) NMR δ 9.58 (d, ^3J = 6.8 Hz, 1H), 9.36 (d, ^3J = 6.0 Hz, 1H), 8.86−8.79 (4 line, m, 4H), 8.73 (d, ^3J = 8.5 Hz, 1H), 8.67−8.66 (2 line, m, 4H), 8.57 (s, 1H), 8.49 (d, ^3J = 7.6 Hz, 1H), 8.42 (d, ^3J = 8.0 Hz, 1H), 8.23−8.11 (8 line, m, 8H), 8.05 (d, ^3J = 5.0 Hz, 1H), 8.01−7.93 (8 line, m, 4H), 7.82−7.79 (5 line, m, 3H), 7.63−7.50 (9 line, m, 5H), 7.41 (t, ^3J = 6.6 Hz, 1H), 1.46 (s, 18H). $^{13}C\{^1H\}$ (100.6 MHz) δ 165.9, 165.8, 158.2, 158.2, 158.1, 157.2, 154.0, 153.6, 153.0, 152.8, 152.6, 152.5, 152.4, 151.4, 151.2, 150.1, 140.9, 139.7, 138.9, 138.9, 138.8, 137.9, 130.1, 128.7, 128.6, 128.0, 125.9, 125.8, 125.6, 125.3, 125.3, 125.2, 124.8, 124.7, 124.6, 121.9, 121.8, 121.3, 121.3, 120.8, 120.3, 97.6, 54.9, 36.7. ES-MS (CH_3CN) *m/z* 1380.2 (100%, $[M-PF_6]^+$), 617.5 (40%, $[M-2PF_6]^{2+}$). Anal. Calcd for $C_{62}H_{54}F_{12}N_{10}P_2PtRu$ (M_r = 1525.3): C, 48.82; H, 3.57; N, 9.18. Found: C, 48.82; H, 3.57; N, 9.18.

Preparation of PtRu$_2$. After the dissolution of [(dbbpy)-Pt(ebpy)$_2$] (0.050 g, 0.061 mmol) in a mixture of ethanol (20 mL) and dichloromethane (20 mL), 2 equiv of [Ru(bpy)]$Cl_2 \cdot 2H_2O$ (0.063 g, 0.119 mmol) were added. After stirring at 70 °C for two days, the solvent was removed under reduced pressure, and the residue was purified by column chromatography using silica as solid support and a gradient of aqueous sutured solution of K_2CO_3 (0.01−0.05%) in mixture of acetonitrile 85% and water 15% as mobile phase. The solid residue was dissolved in minimum of dimethylformamide (2 mL), and dropwise into an aqueous solution (2 mL) containing KPF_6 (0.120 g). The complex was recovered by filtration over paper, washed with water (3 × 100 mL) and the red solid dried under high vacuum. Ultimate recrystallization by slow evaporation of dichloromethane from a dichloromethane/cyclohexane solution afforded complex [(dbbpy)Pt(ebpy)$_2$Ru(bpy)$_2$)$_2$]$(PF_6)_4$ PtRu$_2$ (0.066 g, 49%). ^{1}H (200.1 MHz, acetone) NMR δ 9.18 (d, ^3J = 5.8 Hz, 2H), 8.84−8.69 (11 line, m, 13H), 8.21−7.98 (13 line, m, 22H), 7.84 (s, 2H), 7.72−7.50 (12 line, m, 13H), 1.46 (s, 18H). FTIR (ATR): ν = 3084 (m), 2959 (m), 2114 (m, $\nu_{C'C}$), 1723 (m), 1618 (m), 1601 (m), 1587 (m), 1463 (m), 1446 (m), 1240 (m), 831 (s), 792 (m). ESI-MS (CH_3CN) *m/z* 2083.2 ($[M-PF_6]^+$, 100), 969.0 ($[M-2PF_6]^{2+}$, 80); 598.1 ($[M-3PF_6]^{3+}$, 50). Anal. Calcd for $C_{82}H_{70}F_{24}N_{14}P_4PtRu_2$ (M_r = 2228.6): C, 44.19; H, 3.17; N, 8.80. Found: C, 43.78, H, 2.93, N, 8.49.

Preparation of PtOs$_2$. After the dissolution of [(dbbpy)-Pt(ebpy)$_2$] (0.050 g, 0.061 mmol) in a mixture of ethanol (50 mL) and of dichloromethane (30 mL), 1 equiv of [Os(bpy)]Cl_2 (0.034 g, 0.061 mmol) was added. The solution was stirring at 80 °C overnight, and the solvent was removed under reduced pressure. The solid residue was dissolved in a mixture of water and acetone containing KPF_6 (0.250 g); after stirring the solvent was removed under reduced pressure. The residue was extracted with acetone and the dark solid dried under high vacuum. Purification was ensured by column chromatography using alumina as solid support and a gradient of methanol (0.5−3%) in dichloromethane as mobile phase. Ultimate recrystallization in acetone/pentane afforded complex [(dbbpy)Pt(ebpy)$_2$(Os(bpy)$_2$)$_2$]$(PF_6)_4$ PtOs$_2$ (0.060 g, 42%).^{1}H (400.1 MHz, acetone) NMR δ 9.62 (d, ^3J = 6.1 Hz, 1H), 9.38 (d, ^3J = 5.7 Hz, 1H), 8.87−8.82 (3 line, m, 6H), 8.77 (d, ^3J = 7.4 Hz, 1H), 8.71−8.67 (3 line, m, 4H), 8.57 (s, 1H), 8.50 (d, ^3J = 7.2 Hz, 1H), 8.43 (d, ^3J = 8.2 Hz, 1H), 8.14 (d, ^3J = 5.3 Hz, 1H), 8.05−7.92 (9 line, m, 18H), 7.82−7.79 (5 line, m, 4H), 7.71 (s, 1H), 7.54−7.39 (15 line, m, 12H), 1.48 (s, 18H). FTIR (ATR): ν = 3073 (m), 2960 (m), 2113 (m, $\nu_{C'C}$), 1618 (m), 1610 (m), 1585 (m), 1461 (m), 1421 (m), 1243 (m), 837 (s), 763 (m). ESI-MS (CH_3CN) *m/z* 2264.3 ($[M-PF_6]^+$, 100), 1058.4 ($[M-2PF_6]^{2+}$, 60); 658.1 ($[M-3PF_6]^{3+}$, 20). Anal. Calcd for $C_{82}H_{70}F_{24}N_{14}Os_2P_4Pt$ (M_r = 2406.92): C, 40.92; H, 2.93; N, 8.15. Found: C, 40.65; H, 2.71; N, 7.78.

Preparation of PtRuOs. The preparation began with the dissolution of [(dbbpy)Pt(ebpy)$_2$Ru(bpy)$_2$]$(PF_6)_2$ (0.035 g, 0.030 mmol) in ethanol (25 mL), followed by the addition of [Os(bpy)]Cl_2 (0.015 g, 0.030 mmol). The solution was stirring at 80 °C overnight and the solvent was removed under reduced pressure. The solid residue was dissolved in a mixture of water and acetone containing KPF_6 (0.100 g); after stirring the solvent was removed under reduced pressure. The residue was extracted with acetone and the dark solid dried under high vacuum. Purification was ensured by column chromatography using alumina as a solid support and a gradient of methanol (0.5−2%) in dichloromethane as a mobile phase. Ultimate recrystallization in acetone/pentane afforded complex [(dbbpy)Pt(ebpy)$_2$Ru(bpy)$_2$-Os(bpy)$_2$]$(PF_6)_4$ PtRuOs (0.021 g, 29%). ^{1}H (400.1 MHz, acetone) NMR δ 10.49 (dd, ^3J = 20.6 Hz,^3J = 6.0 Hz, 1H), 10.34−10.11 (8 line, m, 1H), 10.02−9.62 (12 line, m, 2H), 9.53−9.43 (7 line, m, 1H), 9.13−9.01 (11 line, m, 2H), 8.92−8.64 (24 line, m, 7H), 8.38−7.67 (39 line, m, 25H), 7.59−7.34 (18 line, m, 8H), 7.15−6.86 (13 line, m, 2H), 6.86−6.48 (18 line, m, 3H), 1.46 (s, 18H). ESI-MS (CH_3CN) *m/z* 2174.5 ($[M-PF_6]^+$, 100), 1014.7 ($[M-2PF_6]^{2+}$, 50); 628.2 ($[M-3PF_6]^{3+}$, 30), 435.0 ($[M-4PF_6]^{4+}$, 10). Anal. Calcd for $C_{82}H_{70}F_{24}N_{14}P_4OsPtRu$ (M_r = 2317.76): C, 42.49; H, 3.04; N, 8.46. Found: C, 42.11; H, 2.69; N, 8.21.

Cyclic Voltammetry. Electrochemical studies employed cyclic voltammetry with a conventional three-electrode system using a BAS CV-50W voltammetric analyzer equipped with a Pt disk (2 mm^2) working electrode and a silver wire counter-electrode. Ferrocene was used as an internal standard and was calibrated against a saturated calomel reference electrode (SCE) separated from the electrolysis cell by a glass frit presoaked with electrolyte solution. Solutions contained the electro-active substrate in deoxygenated and acetonitrile-containing doubly recrystallized tetra-*n*-butylammonium hexafluorophosphate (0.1 M) as a supporting electrolyte. The quoted half-wave potentials were reproducible within $\approx$ 10 mV. No correction from cell resistance has been made.

Crystal Data for Compound Pt. $C_{42}H_{38}N_6Pt$, CH_2Cl_2, C_6H_{12}, CH_3OH, M = 636.56, yellow prism, size 0.18 × 0.26 × 0.29 mm, λ= 0.7107 Å, 293 K, Triclinic, space group $P\bar{1}$, a = 13.383(1) Å, b = 13.710(1) Å, c = 14.576(3) Å, α = 80.24 (3)°, β = 86.36(3), γ = 61.93 (4)° V = 2325.3(10) Å^3, Z = 2, d_c= 1.461 g·cm^{-3}, $F(000)$ = 1036 μ = 3.18 mm^{-1}, 16 783 data measured to θ_{max} = 24.5° of which 7473 unique* (R_{int} = 0.0416) and 5647 observed with $I > 2\sigma(I)$. Completeness to θ_{max} = 97.2%, 497 parameters with 114 restraints, R1 = 0.043(0.067), wR2 = 0.102(0.112) (All data 7471 data, *Friedel separated) S = 0.988, final difference max peak/hole = 0.655/−1.063 e·Å^{-3}. Diffraction data were collected at ambient temperature on an Enraf-Nonius Kappa-CCD diffractometer using graphite-monochromated Mo Kα (λ = 0.7107 Å) radiation. A preliminary orientation matrix and unit cell parameters were determined from a 10° φ scan of 1° oscillation, followed by spot integration and least-squares refinement. The strategy[23,24] for complete data collection in a triclinic system up to a resolution of θ = 24.1° proposed a φ scan of a 183° range with 2° oscillation, followed by three ω scans of successive lengths: 43.4, 97.5° twice. ≪Dezingering≫ was accomplished by measuring each frame twice with an exposure of 30 s per frame. The detector was put at the distance of 31 mm from the crystal. Data reduction and cell dimension postrefinement were performed using the *HKL2000* package.[24] Correction for absorption mainly due to Pt atoms was used as implemented within *SCALEPACK*.[24]

The structure was solved using direct methods (*SHELX-S97*),[25] and all non-hydrogen atoms were refined with anisotropic displacement parameters using *SHELX-L97*[25] by full-matrix least-squares on F^2 values. All hydrogen atoms were located on difference-Fourier syntheses and were refined with a riding model and with U_{iso} set to 1.2 times that of the attached aromatic C atom (1.5 when methyl group). The asymmetric unit comprises one molecule of compound and one solvent dichloromethane molecule. The *PLATON*[26]*SQUEEZE* procedure was employed to treat regions of diffuse solvent, which could not be sensibly modeled in terms of atomic sites. Their contribution to the diffraction pattern was removed and modified F_o^2 written to a new HKL file. The number of electrons thus located, 133.2 per unit cell, was included in the formula, formula weight, calculated density, μ, and F(000). This residual electron density was potentially assigned to one molecule of cyclohexane (48 e-) and one molecule of methanol (18 e-).

Structural data have been deposited with the Cambridge Crystallographic Data Centre (CIF file) as supplementary publication number CCDC 679537. Copies of the data can be obtained free of charge, on application to CCDC, 12 Union Road, Cambridge CB21, EZ, UK [fax: +44−1−223−336−033 or e-mail: deposit@ccdc.cam.ac.uk]

Optical Spectroscopy. UV−vis absorption spectra of CH_3CN dilute solutions (2 × 10^{-5} M) of the complexes were obtained with Uvikon 933 or Perkin-Elmer Lambda 950 spectrophotometers. The luminescence spectra for O_2-free solutions at room temperature (absorbance <0.15 at the excitation wavelength) and at 77 K were measured by using a Spex Fluorolog II spectrofluorimeter with excitation wavelengths λ_{exc} = 376, 452, and 600 nm, for excitation of Pt/Ru/Os centers, Ru/Os centers, and solely Os centers, respectively. Luminescence quantum efficiencies (ϕ_{em}) were evaluated by comparing wavelength-integrated intensities (I) with reference to $[Ru(bpy)_3]Cl_2$ (ϕ_r = 0.028, air-equilibrated water),[27] quinine sulfate (ϕ_r = 0.546, H_2SO_4 1 N, air-equilibrated),[28] and $[Os(ttpy)_2]^{2+}$ (ϕ_r = 0.021, O_2-free butyronitrile, ttpy is tolylterpyridine),[29] by using the following equation,[30]

$$\phi_{em} = \frac{A_r n^2 I}{n_r^2 I_r A}\phi_r \qquad (1)$$

where A and n are absorbance values (<0.15) at the employed excitation wavelength and refractive index of the solvent, respectively. Band maxima and relative luminescence intensities are obtained with uncertainty of 2 nm and 20%, respectively. Excitation spectra were also obtained at the different luminescence peaks; however, they were of limited use given the extensive overlap of the PtLCT, RuLCT, OsLCT, and ILCT absorption features. The luminescence lifetimes of the complexes were obtained with an IBH 5000F single-photon equipment using nanoled excitation sources at 373 and 465 nm for excitation of different proportions of Pt/Ru/Os and Ru/Os centers in the mixed metal complexes, as described in the text and footnotes of Table 2; a nanoled at 560 nm was employed to excite the Os center in the same complexes, respectively. Analysis of the luminescence decay profiles against time was accomplished by using software provided by the manufacturers. The estimated error on lifetimes is 10%. The working temperature was either 295 ± 2 K (1 cm square optical cells employed) or 77 K (with samples contained in capillary tubes immersed in liquid nitrogen).

(23) *Collect In*; Nonius B.V., 1998.
(24) Otwinovski, Z.; Minor, W. In *Methods in Enzymology*; Academic Press: New York, 1997; pp 307−326.
(25) Sheldrick, G. M. *Program for the Refinement of Crystal Structures from Diffraction Data*; Göttingen, 1997.
(26) Spek, A. L. *PLATON, A Multipurpose Crystallographic Tool*, Utrecht University: Utrecht, The Netherlands, 2004.
(27) Nakamaru, K. *Bull. Chem. Soc. Jpn.* **1982**, *55*, 2697–2705.
(28) Eaton, D. F. *Pure Appl. Chem.* **1988**, *60*, 1107–1114.
(29) Sauvage, J. P.; Collin, J. P.; Chambron, J. C.; Guillerez, S.; Coudret, C.; Balzani, V.; Barigelletti, F.; Decola, L.; Flamigni, L. *Chem. Rev.* **1994**, *94*, 993–1019.
(30) Demas, J. N.; Crosby, G. A. *J. Phys. Chem.* **1971**, *75*, 991–1024.

Table 1. Electrochemical Data for the Pt/Ru/Os Complexes and Appropriate References[a]

	$E^{0\prime}$(ox, soln) (V), ΔE (mV)	$E^{0\prime}$(red, soln) (V), ΔE (mV)
Pt	+1.37 (irrev, $I_a/I_c \approx 0$)	−1.43 (70)
$PtCl_2$	+1.38 (irrev, $I_a/I_c \approx 0$)	−1.38 (80)
PtRu	+1.32[b]	−1.33 (60), −1.37 (70), −1.61 (60)
$PtRu_2$	+1.32[b]	−1.34 (60), −1.39 (60), −1.63 (60)
Ru	+1.40 (60)	−1.17 (60), −1.55 (100)[c]
$PtOs_2$	+0.90 (60)	−1.26 (60), −1.40 (60), −1.60 (70)
Os	+0.96 (60)	−1.11 (70), −1.47 (80)
PtRuOs	+1.34 (60), +0.91 (60)	−1.32 (70), −1.42 (120),[c] −1.60 (80)

[a] Potentials determined by cyclic voltammetry in deoxygenated CH_2Cl_2 solution, containing 0.1 M $TBAPF_6$, at a solute concentration of ca. 1.5 mM and at room temperature. Potentials were standardized versus ferrocene (Fc) as an internal reference and converted to the SCE scale assuming that $E_{1/2}$ (Fc/Fc^+) = +0.38 V (ΔE_p = 60 mV) vs SCE. Uncertainty in half-wave potentials is ± 15 mV, and the indicated potential corresponds to a single electron transfer unless otherwise noticed. For irreversible processes, the peak potentials (E_{ap}) are quoted. [b] The visibility is perturbed by adsorption of the complex on the electrolyte surface. [c] Two-electron process.

Results and Discussion

Synthesis. To prepare the polynuclear complexes sketched in Charts 1 and 2, we envisaged two strategies. The first one was based on the cross-coupling of the monoethynyl derivatives Ru or Os with the [(dbbpy)Pt(Cl)$_2$] precursor, $PtCl_2$. Unfortunately, oxidative homocoupling of the Ru and Os was observed owing to the need of CuI to catalyze the cross-coupling with $PtCl_2$. These reactions were very efficient despite the absence of oxygen. After some experimentation, we succeeded in preparing the [(dbbpy)Pt(ebpy)$_2$] complex Pt in 78% isolated yield by cross-coupling the acetylene precursor ebpy (excess) with $PtCl_2$ under anaerobic conditions using CuI (10 mol%) as catalyst in a mixture of DMF and triethylamine (10 vol %). The corresponding PtRu and $PtRu_2$ complexes were prepared from the metallo-ligand Pt and stoichiometric amounts of $[Ru(bpy)_2Cl_2]\cdot 2H_2O$ in refluxing ethanol. When 1 equiv of the precursor was used, 67% of PtRu was isolated with 15% of $PtRu_2$.The synthesis of $PtRu_2$ was increased to 49% by the use of 2.2 equiv of the Ru precursor over longer reaction times. In this case, the PtRu was isolated with less than 10% yield. All compounds were systematically purified by column chromatography on alumina as a solid phase and CH_2Cl_2/CH_3OH as mobile phase. Recrystallization in adequate solvents afforded the analytically pure samples. The molecular structures of the complexes were unambiguously assigned by NMR spectroscopy and electro-spray mass analysis in a positive mode.

X-ray Analysis of [(dbbpy)Pt(ebpy)$_2$] Pt. The X-ray structure of complex Pt-dichloromethane solvate (grown from $CH_2Cl_2/C_6H_{12}/CH_3OH$) was determined, revealing a quasi-undistorted square-planar geometry of the Pt(II) center, the maximum of rms deviation out of the Pt(bpy) mean plane being 0.044Å (for the Pt atom, Figure 1). The overall molecule appears to be quasi-planar with the two uncomplexed bipyridyl fragments containing N3/N4 and N5/N6 barely twisted from the plane of the 2,2′-bipyridyl Pt fragment by 16.8 and 7.8°, respectively. Both bipyridine substituents have nitrogen atoms in a transoid position and are slightly distorted as shown by the ring dihedral angles of 4.8 and 8.2°, respectively. This transoid arrangement is due to the nitrogen lone pairs repulsion and was previously observed in oligopyridine derivatives.[31] Platinum bipyridine-nitrogen atoms and Pt-alkyne distances are in keeping with related square planar complexes.[32,33] Crystal packing is described in the SI section.

Redox Properties. The electrochemical properties of the complexes were determined by cyclic voltammetry in dichloromethane solution. Table 1 lists the potentials (relative to the SCE reference electrode) for the waves that were observed in the +1.6 to −2.2 V window. For the platinum precursors Pt and $PtCl_2$, an irreversible anodic wave was observed around +1.37 V that is due to the Pt oxidation.[33]

For the Ru and Os references, the metal centered oxidation (M(II)/M(III)) is found at +1.40 V and +0.96 V, respectively. The Ru(II/III) wave is shifted slightly negative by 80 mV in PtRu and $PtRu_2$ compared to Ru; this shift likely reflects the fact that Pt(dbbpy) fragment is slightly electron donating. Likewise the Os(II/III) oxidation is shifted negative by 60 mV in $PtOs_2$ compared to Os. The presence of two Ru or Os centers does not change the oxidation potentials of the respective metals, and a single, multielectron wave is observed for the Ru(II/III) and Os(II/III) couples. This indicates that the electronic coupling between the metal centers is weak, that is, within 15 mV, the uncertainty for the electrochemical data, Table 1. However, this corresponds to ca. 120 cm^{-1} that by contrast is to be regarded as a strong coupling in view of photoinduced processes like energy transfer (below).[34] In the mixed PtRuOs triad, both metal oxidations are clearly defined and little perturbed compared to the reference complexes. For PtRu, $PtRu_2$, PtOs, $PtOs_2$, and PtRuOs, there is no clear indication of Pt-centered oxidation.

The Pt and $PtCl_2$ complexes exhibit one reversible wave in the cathodic branch of the voltammograms that is due to the reduction centered on the coordinated dbbpy ligand.[35,36] Notice that when the two chloro ligands are replaced by ebpy the reduction potential is more cathodic (by 50 mV), reflecting some electronic influence toward the reduction of the dbbpy ligands, which resides at the opposite site.

The first reduction occurs at −1.33 ± 0.1 V in the PtRu, $PtRu_2$, and PtRuOs cases and at −1.26 V in the $PtOs_2$ case. This suggests that in all of these complexes the first reduction is localized on the ebpy. Moreover, there are significant differences in the potentials of the first reduction compared to the first reduction of Ru (Δ = 170 mV) and Os (Δ = 130 mV), which again reflects the significant electron donating ability of the Pt(dbbpy) moiety.

(31) Drew, M. G. B.; Hudson, M. J.; Iveson, P. B.; Russell, M. L.; Liljenzin, J. O.; Skalberg, M.; Spjuth, L.; Madic, C. *J. Chem. Soc., Dalton Trans.* **1998**, 2973–2980.
(32) Yam, V. W. W.; Tang, R. P. L.; Wong, K. M. C.; Cheung, K. K. *Organometallics* **2001**, *20*, 4476–4482.
(33) Hua, F.; Kinayyigit, S.; Rachford, A. A.; Shikhova, E. A.; Goeb, S.; Cable, J. R.; Adams, C. J.; Kirschbaum, K.; Pinkerton, A. A.; Castellano, F. N. *Inorg. Chem.* **2007**, *46*, 8771–8783.
(34) Barigelletti, F.; Flamigni, L. *Chem. Soc. Rev.* **2000**, *29*, 1–12.
(35) Adams, C. J.; Raithby, P. R. *J. Organomet. Chem.* **1999**, *578*, 178–185.
(36) Adams, C. J.; James, S. L.; Liu, X. M.; Raithby, P. R.; Yellowlees, L. J. *J. Chem. Soc.-Dalton Trans.* **2000**, 63–67.

Table 2. Absorption and Emission Properties[a]

	Absorption	Emission, 295 K			Emission, 77 K		
	λ_{max}(nm), ε($M^{-1}cm^{-1}$)	λ_{em}(nm)	ϕ_{em}	τ_{em}(μs)	λ_{em}(nm)	τ_{em}(μs)	E(eV)
Pt[b]	319 (39 200), 376 (10 240)	513	0.175	4.7	522	58.0	2.38
Ru[c]	288 (70 000), 452 (11 240)	634	0.054	0.80	615	4.6	2.02
$[Ru(bpy)_3]^{2+}$[d]	285 (87 000), 452 (14 000)	626	0.062	0.90			
PtRu[e]	288 (91 000), 376 (35 600), 452 (13 700)	610[b], 610[c]	0.092[b], 0.092[c]	1.60[b], 1.49[c]	596[b], 596[c]	4.7[b], 4.4[c]	2.08
$PtRu_2$[e]	288 (129 900), 366 (52 600), 454 (24 100)	612[b], 612[c]	0.084[b], 0.082[c]	1.58[b], 1.44[c]	599[b], 599[c]	4.3[b], 4.0[c]	2.07
Os[c]	291 (77 200), 449 (11 900), 482 (11 000), 580 (3900)	766	5.4×10^{-4}	0.016	~750	2.3	~1.65
$[Os(bpy)_3]^{2+}$[f]	290 (78 000), 478 (11 100), 579 (3300)	743	5.0×10^{-3}	0.060			
$PtOs_2$[e]	291 (186 000), 374 (60 800), 483 (24 300), 580 (7400)	722[b], 722[c]	6.0×10^{-3}[b], 2.8×10^{-3}[c]	0.060[b], 0.029[c]	721[b], 721[c]	~1.0[b], 1.4[c]	1.72
PtRuOs[g]	291 (159 800), 366 (34 640), 452 (23 500), 582 (4100)	612[b,i]	0.008[b,i]	1.24[b,i]	597[b,i]	4.1[b,i]	2.08
		612[c,i]	0.015[c,i]	1.0[c,i]	599[c,i]	4.7[c,i]	
		726[h]	9.6×10^{-4}[h]	0.018[h]	710[h]	1.4[h]	1.75

[a] In O_2-free CH_3CN solutions, the last column lists the energy content of the emission level, E. [b] λ_{exc} = 376 nm for the emission spectra and 373 nm for the lifetimes. [c] λ_{exc} = 452 nm for the emission spectra and 465 nm for the lifetimes. [d] Ref 18. [e] For PtRu, $PtRu_2$, and $PtOs_2$ the luminescence spectra were obtained upon excitation both at λ_{exc} = 376 and 452 nm, whereas for the luminescence lifetimes λ_{exc} = 373 and 465 nm were employed; this allows predominant excitation of the Pt-based chromophore and selective excitation of the Ru- or Os-based chromophore, respectively (text). [f] Ref 40. [g] For PtRuOs, the luminescence spectra were obtained upon excitation at λ_{exc} = 376, 452, and 600 nm, whereas for the luminescence lifetimes λ_{exc} = 373, 465, and 560 nm were employed; this allows predominant excitation of the Pt-based chromophore, 1:1 excitation of Ru- and Os-based chromophores, and selective excitation of the Os-based chromophore, respectively (text). [h] λ_{exc} = 600 nm for the emission spectra and 560 nm for the lifetimes. [i] Too weak to be determined.

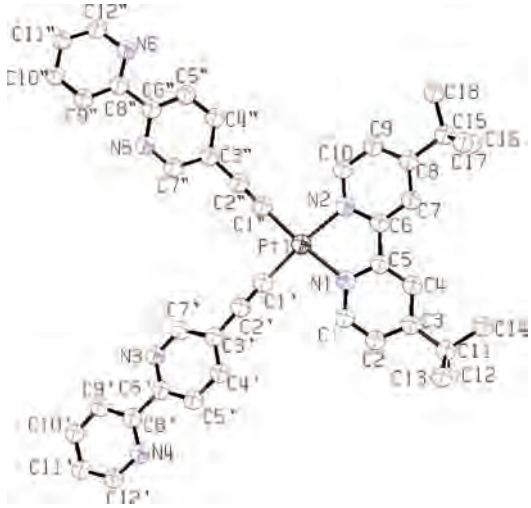

Figure 1. Ortep view of Pt (50% probability displacement ellipsoids) with one disordered *tert*-butyl C(15) refined with two sites rotated approximately by 60° (not shown for clarity). Selected bond lengths and angles: Pt(1)—N(1) 2.065(5), Pt(1)—N(2) 2.070(6), Pt(1)—C(1′) 1.951(7), Pt(1)—C(1″) 1.952(7), N(1)—Pt(1) —N(2) 79.0(2)°, C(1′)—Pt(1)—C(1″) 89.5(3)°.

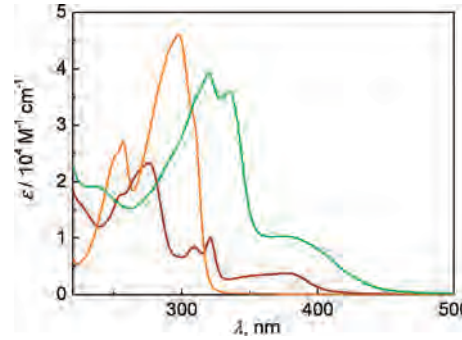

Figure 2. Ground-state absorption spectra of Pt (green line), $PtCl_2$ (wine line), and twice the absorption spectrum of ebpy (orange line) obtained in CH_3CN.

The second and third reduction waves could not be assigned due to the presence of the dbbpy and the unsubstituted bipyridine ligands surrounding the Ru and Os centers. These cathodic potentials are very similar along the PtRu, $PtRu_2$, $PtOs_2$, and PtRuOs series of complexes but significantly different compared to the Ru and Os mononuclear complexes.

Optical Absorption Properties. Figures 2, 3, and 4 show absorption spectra obtained in CH_3CN for Pt, Ru, Os, $PtRu_2$, $PtOs_2$, and PtRuOs. Absorption data are listed in Table 2. Pt can be considered a model for the same unit present in the dyads and triads studied, and it is interesting to compare its absorption properties with those of [Pt(dbbpy)Cl_2], $PtCl_2$,[37] and HC≡C(bpy), ebpy, Figure 2. Clearly, the spectrum of Pt does not overlap with the sum of the spectra of the model components. In particular, the band system below 330 nm, attributable to $\pi\pi^*$ transitions centered on the ligands, is red-shifted compared to the same transitions observed in the spectra of $PtCl_2$ and ebpy. The lowest energy band of Pt, peaking at 376 nm, appears at the same wavelength of the $PtCl_2$ complex (Figure 2) and is to be ascribed to Pt → dbbpy ^{1}MLCT transitions; however, it shows an increase in the epsilon value of about 3 times with respect to $PtCl_2$. The absorption profiles of Figure 2 illustrate the influence of the direct coordination of ebpy to the metal in the Pt complex. Even if the band at 376 nm is assigned of MLCT nature like for the $PtCl_2$ case (i.e., with an electron promoted from the d orbital of the metal to the π^* orbital of dbbpy), in the case of Pt the involvement of the distant bipyridine units of the acetylenic fragments cannot apparently be excluded; however, this is not the case (below).

In the top panel of Figure 3, are compared the ground-state absorption spectra of Pt, Ru, and $PtRu_2$, Table 2 collects concerned data.[17] The absorption properties of Ru, the Ru-based component of PtRu and $PtRu_2$, provide useful hints regarding the electronic interactions within the multinuclear complexes. The lowest-energy absorption peak of Ru is practically coincident with that of the prototypical $[Ru(bpy)_3]^{2+}$ complex,[18] (Table 2) suggesting a minor effect by the acetylide moiety appended at the 5 position of a bpy ligand. For both PtRu and $PtRu_2$, the absorption maximum of the lowest-energy ^{1}MLCT band, falling at 452 and 454

(37) Miskowski, V. M.; Houlding, V. H.; Che, C. M.; Wang, Y. *Inorg. Chem.* **1993**, *32*, 2518–2524.

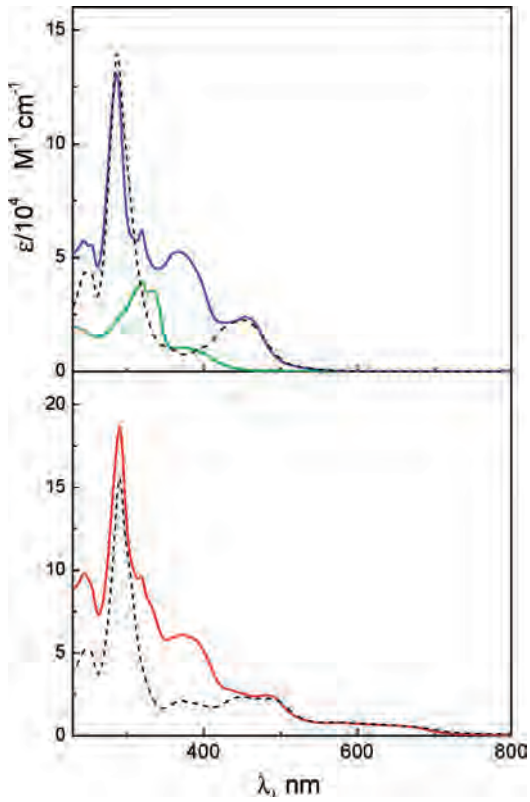

Figure 3. Ground-state absorption spectra, CH_3CN solvent. Top panel, $PtRu_2$ (blue line) as compared with the components, Pt (green line), and twice Ru (black dashed line). Bottom panel, $PtOs_2$ (red line) and twice Os (black dashed line).

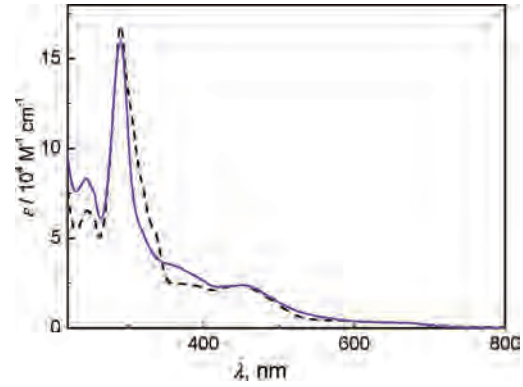

Figure 4. Absorption spectra of PtRuOs (blue line) as compared with the sum (dashed line) of the Pt, Ru, and Os components, solvent CH_3CN.

nm, respectively (Table 2), keeps practically unchanged with respect the cases of both $[Ru(bpy)_3]^{2+}$ and Ru. The concerned absorption intensity for this band is $\epsilon = 13\,700$ and $24\,100$ M^{-1} cm^{-1} for PtRu to $PtRu_2$, respectively, reflecting the presence of two Ru-based units in the latter case. Likewise, the intensity of the peak at 288−290 nm, of clear attribution as bpy-centered $^1\pi\pi^*$ transitions (Figure 3),[18] reflects the number of coordinated bpy in the dyad and triad. All of this suggests that upon incorporation in PtRu and $PtRu_2$ the $[Ru(ebpy)(bpy)_2]^{2+}$ unit retains to a high degree some of the individual electronic properties. On the other hand, for both PtRu and $PtRu_2$ and with respect to the component Ru- and Pt-based units, a remarkably more intense absorption is registered in the region of the Pt → dbbpy CT transitions, 376 nm ($\epsilon = 35\,600$ M^{-1} cm^{-1}) and 366 nm ($\epsilon = 52\,600$ M^{-1} cm^{-1}), respectively. For these multinuclear complexes, the terminal charged centers, the $[Ru(bpy)_2]^{2+}$ units, should reduce the electron density at the Pt(II) center, in turn inducing a blue shift of the Pt → dbbpy CT transitions, as actually observed for $PtRu_2$. To notice that this excludes a role for Pt → ebpy CT transitions, that would appear red-shifted.

Enhanced absorption intensities have been reported in some cases for the Pt → dbbpy CT transition;[6,38] however, for PtRu and $PtRu_2$ the observed band in this region is too intense to be of neat MLCT character, whose intensity is typically of the order of $1-2 \times 10^4$ M^{-1} cm^{-1} or less.[2,18,39] Thus, for PtRu and $PtRu_2$ the intense absorption bands falling at 376 and 366 nm, respectively, are likely due to mixed Ru-based (likely of ^{1}RuLCT character[18]), ^{1}Pt → dbbpy CT and ^{1}ILCT transitions, the last possibly involving the ebpy sites (also, ^{1}MMLCT transitions could be envisaged).[2,17] Consistent with this, first reduction in the dyad and triad appears localized at the ebpy fragment (−1.17, −1.33, and −1.34 V for Ru, PtRu, and $PtRu_2$, respectively; Table 1), which suggests the possibility of ILCT interactions involving the C≡C−bpy moiety of the investigated polymetallic complexes.[17]

The absorption spectrum of $PtOs_2$ is shown in the bottom panel of Figure 3 and is compared with those of the Os components; Table 2 collects concerned data. The absorption spectrum of the dyad PtOs is not available due to the poor stability of this array in acetonitrile. The absorption features of Os are quite similar to those of the widely studied $[Os(bpy)_3]^{2+}$ complex, also listed in Table 2.[40,41] Of relevance is the extension of the absorption profile to include the region 550−750 nm, due to direct absorption from the ground-state to the ^{3}MLCT level, a heavy atom effect from the Os(II) center. From inspection of the figure, it emerges that also in this case in the region below 350 nm and in the region corresponding to the MLCT transitions of the Os-based moiety (430−750 nm) there is a good agreement between the spectrum of the triad and the sum of the spectra of the components. In contrast, for the region 350−400 nm the band with maximum at 374 nm is characterized by an extinction coefficient twice the value of the sum of the Pt and Os components. As discussed above for the cases of PtRu and $PtRu_2$, in addition to Os-based transitions, the band at 374 nm includes contributions from both ^{1}Pt → dbbpy CT and ^{1}ILCT transitions.

The absorption spectrum of the triad PtRuOs is shown in Figure 4 together with the sum of the spectra of the three components, Pt, Ru, and Os; data are displayed in Table 2. The spectrum of PtRuOs in this case reasonably matches the superimposition of the spectra of the component models, apart the region 350−400 nm, where a shoulder with

(38) Hua, F.; Kinayyigit, S.; Cable, J. R.; Castellano, F. N. *Inorg. Chem.* **2006**, *45*, 4304–4306.
(39) Balzani, V.; Juris, A.; Venturi, M.; Campagna, S.; Serroni, S. *Chem. Rev.* **1996**, *96*, 759–833.
(40) Kober, E. M.; Caspar, J. V.; Lumpkin, R. S.; Meyer, T. J. *J. Phys. Chem.* **1986**, *90*, 3722–3734.
(41) De Cola, L.; Balzani, V.; Barigelletti, F.; Flamigni, L.; Belser, P.; Von Zelewsky, A.; Frank, M.; Vögtle, F. *Inorg. Chem.* **1993**, *32*, 5228–5238.

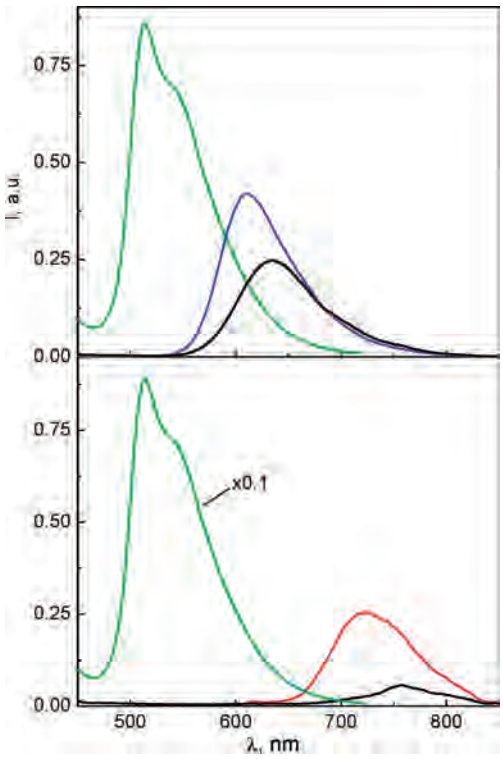

Figure 5. Room-temperature emission spectra upon excitation of isoabsorbing air-free solutions at 376 nm. Top panel, $PtRu_2$ (blue line) and models Pt (green line) and Ru (black line); bottom panel, $PtOs_2$ (red line) and models Pt (green line) and Os (black line).

extinction coefficient 20% higher than the sum of the components is observed. Therefore, with respect to $PtRu_2$ and $PtOs_2$, for this complex either ^{1}Pt → dbbpy CT or ^{1}ILCT transitions are somewhat weaker. Also in this case the presence of the Os(II) center results in an absorption band extending till 750 nm with an extinction coefficient reflecting the presence of only one Os-based unit (Table 2).

Luminescence Properties. Figure 5 shows room temperature luminescence profiles for Pt, Ru, Os, $PtRu_2$, $PtOs_2$, and PtRuOs as obtained upon excitation of O_2-free isoabsorbing CH_3CN solutions at 376 nm; luminescence results are collected in Table 2. The luminescence profile of Pt is somewhat resolved, Figure 5, and the emission lifetime $\tau_{em} = 4.7\ \mu s$ is substantially larger than for other Pt(II) acetylide complexes exibiting ^{3}PtLCT luminescence.[2–4,6] In addition, the radiative rate constant, $k_r = 3.7 \times 10^4\ s^{-1}$ is lower by 1 order of magnitude than that typical of ^{3}PtLCT emissions,[2] suggesting that the excited-state responsible for the emission in Pt includes $^3\pi\pi^*$ contributions; $k_r = \phi_{em}/\tau_{em}$. This is supported by the 77 K emission results, Table 2, because the emission peak falls at 522 nm (i.e., red-shifted with respect to the room temperature value, 513 nm) and the lifetime is 58 μs, too long for a neat ^{3}MLCT emission.[2]

The luminescence properties of Ru and Os are easily identified of ^{3}MLCT nature upon comparison with those of $[Ru(bpy)_3]^{2+}$,[18] and $[Os(bpy)_3]^{2+}$,[40] respectively (Table 2). To notice that the emission peak exhibited by Os lies at lower energy than for $[Os(bpy)_3]^{2+}$, $\lambda_{em} = 766$ and 743 nm, respectively. For Os, this occurrence might explain the lower luminescence intensity, ϕ_{em}, and shorter lifetime, τ_{em} (Table 2), possibly based on energy gap law effects.[40]

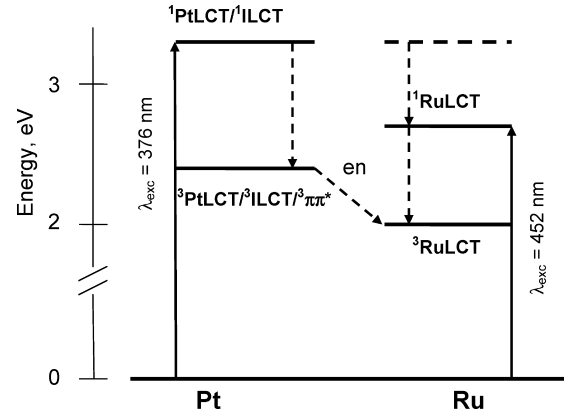

Figure 6. Energy layout for the Pt-, Ru-based and ILCT levels in $PtRu_2$ (a similar picture holds for PtRu); en = energy transfer.

We have obtained the emission properties of the mixed-metal complexes investigated here using different excitation wavelengths. As far as possible, our approach was aimed at selecting transitions localized at the various Pt(II), Ru(II), and Os(II) centers. Accordingly, for PtRu and $PtRu_2$ we employed two excitation wavelengths (Table 2).[17] In one case, use of $\lambda_{exc} = 452$ nm (and 465 nm for the lifetime, see the experimental section) allows excitation of only the Ru-based unit. In contrast, with $\lambda_{exc} = 376$ nm (and 373 nm for the lifetime) one populates ^{1}PtLCT, ^{1}ILCT, and Ru-based states. Consideration of the value for the extinction coefficient of Pt and Ru at 376 nm (top panel of Figure 3) indicates that, for PtRu, ca. 40% of the light is directly absorbed via ^{1}MLCT transitions, roughly partitioned as 2.6:1 for ^{1}PtLCT (i.e., ^{1}Pt → dbbpy CT) and Ru-based transitions, respectively (accordingly, 60% of the absorbed light is tentatively attributed to ^{1}ILCT transitions). For $PtRu_2$, 38% of the absorbed light yields ^{1}PtLCT and Ru-based states in the ratio 1.2:1, respectively (with 62% of the absorbed light yielding ^{1}ILCT states).

The room-temperature luminescence spectra of $PtRu_2$, Pt, and Ru for isoabsorbing solutions at 376 nm are compared in the top panel of Figure 5.[17] For the triad, no residual Pt-based emission is detected even if a portion of the 376 nm absorption generates ^{1}PtCT states (above). Furthermore, the evaluated luminescence quantum yield, ϕ_{em}, for the detected Ru-based emission in $PtRu_2$ is the same for excitation both at 376 and 452 nm, Table 2. To notice that both ϕ_{em} and τ_{em} are larger in $PtRu_2$ and PtRu than in Ru, a likely consequence of the energy gap law.[40] All of this is consistent with the following picture. For $PtRu_2$, upon excitation at 376 nm the absorbed light yields aliquots of ^{1}PtLCT, ^{1}ILCT, and Ru-based states. The relaxed PtLCT and ILCT (or $\pi\pi^*$) triplet states undergo fast energy transfer to sensitize the ^{3}RuLCT luminescence, which therefore receives contributions from direct 376 nm excitation and sensitization by both the PtLCT and ILCT states. These processes are higly efficient and only Ru-based luminescence is detected; Figure 6 provides an illustration of the involved levels and steps.

From the emission maxima of Pt and $PtRu_2$ as obtained at 77 K (Table 2, and in the Supporting Information), the Pt → Ru energy transfer is estimated to be exothermic by >0.40

eV.[42,43] To describe the energy transfer steps within multimetal assemblies, two mechanisms can be invoked.[34] In one case the intermetal interaction is viewed to take place via dipole−dipole Förster interactions.[44] On the other hand, in the presence of suitable bridging ligands a through bond Dexter mechanism might be appropriate to account for such interactions.[45] The overlap integral between the Pt emission spectrum and the Ru absorption spectrum, as evaluated according to the dipole−dipole mechanism, is $J^F = 8.2 \times 10^{-15}$ cm^3 M^{-1}, whereas that obtained in the frame of a Dexter mechanism is $J^D = 2.4 \times 10^{-5}$ cm (Supporting Information). Accordingly, for the Förster mechanism at an estimated intermetal separation of ca. 9 Å[17] this yields an energy transfer rate constant $k_{en}^F = 1.0 \times 10^8$ s^{-1}. This result accounts well for the observed full quenching of the Pt-based emission in both PtRu and $PtRu_2$ complexes, given that the estimated efficiency of energy transfer is $\eta_{en} = k_{en}^F/(k_{en}^F + \tau_{em}^{-1}) \sim 1$, with the emission lifetime of the donor taken to be that of Pt, $\tau_{em} = 4.7$ μs.

With regard to $PtOs_2$, the use of $\lambda_{exc} = 376$ nm allows population of ^{1}PtLCT and ^{1}ILCT states besides Os-based states (above). From Figure 3, bottom panel, all of this is estimated to result in ca. 15% initial excitation localized at the Pt(II) center and 50% on the ebpy ligands connecting the two metal centers. Selective excitation into an Os(II)-based absorption band was accomplished by using 452 nm for the luminescence spectra and 465 nm for the lifetimes (Experimental Section).

Figure 5 bottom panel displays the room temperature luminescence spectra of $PtOs_2$, Pt, and Os for isoabsorbing solutions at 376 nm. For the triad, no residual Pt-based emission is detected upon 376 nm excitation. Like for the case of $PtRu_2$ seen above, the aliquots of ^{1}PtLCT (15%) and ^{1}ILCT (50%) states produced with $\lambda_{exc} = 376$ nm undergo energy transfer to sensitize the ^{3}OsLCT luminescence, which therefore receives contributions from direct excitation and sensitization by both the PtLCT and ILCT states. Also in this case, no residual Pt-based emission is detected and the evaluated luminescence quantum yield, ϕ_{em}, for the detected Os-based emission looks slightly larger for excitation at 376 than at 452 nm, Table 2, even if the same value would be expected.[46] For $PtOs_2$, an energy scheme analogous to that reported in Figure 6 is expected to hold. From the emission maximum at 77 K of Pt and $PtOs_2$, Table 2, the Pt → Os energy transfer is estimated to be exothermic by >0.60 eV.[47] The Förster and Dexter overlap integrals between the Pt emission spectrum and the Os absorption spectrum are $J^F = 4.7 \times 10^{-14}$ cm^3 M^{-1} and $J^D = 6.4 \times 10^{-5}$ cm, respectively. For the former mechanism, this yields an energy transfer rate constant $k_{en}^F = 5.8 \times 10^8$ s^{-1} at an intermetal separation of ca. 9 Å,[17] accounting for the observed quenching of the Pt-based emission in $PtOs_2$. On the basis of the evaluated overlap integrals, both mechanisms of energy transfer predict a faster step within $PtOs_2$ in comparison with $PtRu_2$ as seen in eq 2 (also see, Supporting Information).

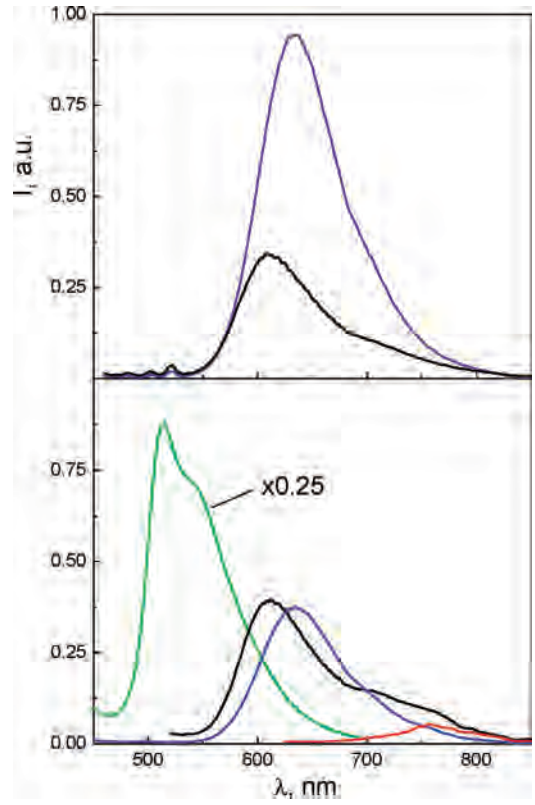

Figure 7. Top panel: Luminescence spectra of isoabsorbing solutions at 452 nm of Ru (blue line) and PtRuOs (black line), CH_3CN solvent; for PtRuOs, this results in 1:1 RuLCT/OsLCT excitation, and the Os-based emission band ($\lambda_{em} = 726$ nm) is hidden by the tail of the scarcely quenched Ru-based emission. Bottom panel: Luminescence spectra of isoabsorbing solutions at 376 nm; given that for PtRuOs this results in 0.35:0.12:0.33 PtLCT/RuLCT/OsLCT excitation, see text, the emission intensity of the Pt, Ru, and Os models has been scaled accordingly, Pt (green line), PtRuOs (black line), Ru (blue line), and Os (red line).

$$\frac{k_{en}^{PtOs_2}}{k_{en}^{PtRu_2}} \cong 3 \div 6 \qquad (2)$$

Bipartion of Energy Transfer in PtRuOs. For PtRuOs, three wavelengths were employed to obtain luminescence spectra, 376, 452, and 600 nm (Table 2). These conditions allowed mixed excitation of Pt/Ru/Os, Ru/Os, and Os-based states, respectively (Figure 4). Comparison of luminescence results obtained with isoabsorbing solutions at 452 nm for Ru and PtRuOs, Figure 7, upper panel, can be performed

(42) A suitable value for the energy level of the ruthenium-based unit of $PtRu_2$ is evaluated from its emission instead than from the emission of Ru.

(43) The energy content of the emissive excited state of platinum is 2.4 eV, as estimated from 77 K measurements of its luminescence spectrum, Table 2, and the lowest-lying redox state for $PtRu_2$ (from oxidation of a ruthenium center and reduction at an ebpy moiety) is >2.6 eV (Table 1). On this basis, for both PtRu and $PtRu_2$, one concludes that photoinduced electron transfer steps cannot compete favorably against photoinduced platinum-to-ruthenium energy transfer.

(44) Förster, T. *Discuss. Faraday Soc.* **1959**, *27*, 7.

(45) Dexter, D. L. *J. Chem. Phys.* **1953**, *21*, 836.

(46) The energy content of the emissive excited state of platinum is 2.4 eV, Table 2, and the lowest-lying redox state of $PtOs_2$ (osmium-based oxidation and ligand-based reduction) lies at ca. 2.16 (Table 1). Thus, upon excitation at 376 nm, photoinduced electron transfer appears exothermic by 0.22 eV. However, we found no evidence for this process in $PtOs_2$, that would manifest by disappearance of the osmium-based luminescence. Remarkably, the same happens for PtRuOs (text).

(47) A suitable value for the energy level of the osmium-based unit of $PtOs_2$ is evaluated from its emission instead than from the emission of Os.

having in mind that for the latter case the obtained excited-state population ratio, ^{1}RuLCT:^{1}OsLCT is evaluated about 1:1. First of all, it is interesting that for PtRuOs, the Ru-based luminescence is not completely quenched, despite the Ru → Os energy transfer step being exothermic by >0.3 eV as evaluated from the 77 K emission maxima (Table 2). In this case, by using eq 3,

$$\frac{I_o}{I} = 1 + k_{en}\tau_0 \quad (3)$$

one can draw an experimental Ru → Os energy transfer rate constant $k_{en}^{RuOs} \sim 4 \times 10^5$ s^{-1}; I_0 and I are the Ru-based intensities of Ru and PtRuOs, respectively, as observed by using $\lambda_{exc} = 452$ nm, and τ_0 is the lifetime of Ru; $I_0/I = 1.4$, in the top panel of Figure 7.[48,49] Given that the two metal centers are ~15 Å from each other,[17] this correspond to a rather slow step in comparison to several documented cases of Ru/Os-polypyridine couples, which suggests that the contribution of the Förster mechanism is negligible.[34,39,50] In addition, on the basis of the fact that the two Ru- and Os-based units for PtRuOs are not directly linked each other, the Dexter contribution is also expected to be negligible.

For PtRuOs, and with reference to the absorption spectra of Figures 3 and 4, use of 376 nm excitation is expected to yield ca. 35% of ^{1}PtLCT levels, against 12 and 33% of Ru- and Os-based levels, respectively; the remaining absorbed light should mainly produce ^{1}ILCT states localized on the two ebpy fragments. The bottom panel of Figure 7 shows the luminescence spectrum of PtRuOs as obtained using λ_{exc} = 376 nm and compares it with the luminescence spectra of Pt (scaled to 35%), Ru (scaled to 12%), and Os (scaled to 33%), with the latter two taken to be approximate models for Ru- and Os-based emissions, respectively. As one can see, for PtRuOs (i) the Pt-based emission completely disappears, a consequence of both Pt → Ru and Pt → Os steps, (ii) the intensity of the Ru-based emission is slightly more than expected on the basis of direct excitation, which means that some amount of Pt → Ru transfer takes place, with the subsequent Ru → Os step being however scarcely effective, (iii) the Os-based emission is the consequence of both Os-based direct excitation and Pt → Os sensitization, with the Ru → Os step playing a minor role (point (ii) above). Figure 8 summarizes the photoinduced steps and energy transfer partitioning taking place in PtRuOs.

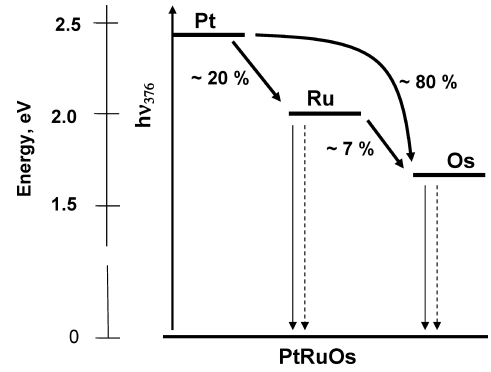

Figure 8. Partition by the indicated fractions of the 376 nm light energy initially absorbed at the Pt unit of PtRuOs; the energy transfer steps are indicated by thick arrows. Radiative (thin full arrow) and nonradiative (thin dashed arrow) processes connecting the Ru- and Os- based excited states to the ground level are also indicated.

Conclusions

In summary, we have accomplished the controlled synthesis of mixed metal Pt-bipyridine-acetylide/Ru- and Os-bipyridine complexes starting from a preorganized square-planar complex in which two free alkyne-bipyridine framents are linked in a cis position. Statistical complexation with the respective metalla-precursor afforded the mixed PtRu complex suitable for the preparation of the PtRuOs triad.

In the $PtRu_2$, $PtOs_2$, and PtRuOs triads, excitation at 376 nm yields considerable fractions of PtLCT and ILCT excited states. For $PtRu_2$ (and PtRu)[17] and $PtOs_2$, respectively, this is followed by effective Pt → Ru and Pt → Os energy transfer and sensitization of the Ru- and Os-based emission, respectively. For the PtRuOs triad as irradiated at 376 nm, we have disantangled the cascade of energy transfer steps by showing that (i) the two competing PtLCT → RuLCT and PtLCT → OsLCT steps take place at different rates, $k_{en}^{PtOs_2} > k_{en}^{PtRu_2}$, (ii) the fraction of energy collected in the terminal Ru-based branch is predominantly disposed to the ground state, with only a small amount being transferred to the Os-based unit, and (iii) the lowest-lying OsLCT level overall collects about 90% of the light initially deposited on the Pt(II)-based unit.

Acknowledgment. The authors thank the CNRS, the Ministère de la Recherche Scientifique, and the ANR FCP-OLEDs N°−05-BLAN-0004-01 for funding; support from Project MACOL PM.P04.010 of CNR, Italy, is also acknowledged.

Supporting Information Available: X-ray analysis of [(dbbpy)-Pt(ebpy)$_2$], Pt; luminescence spectra at 77 K; Pt → Ru/Os energy transfer.This material is available free of charge via the Internet at http://pubs.acs.org.

IC800768V

(48) In this figure, the ruthenium-based emission intensity of Ru must be divided by 2 to obtain ruthenium-based isoabsorbing conditions for the ruthenium-based unit of Ru and PtRuOs at 452 nm.

(49) As noticed above, the emission properties of the ruthenium-based unit are slightly different for the mononuclear complex Ru and the polymetallic species, thus the use of eq 3 only provides approximate figures. To use the more familiar equation $k_{en} = 1/\tau - 1/\tau_0$, ref 34, a suitable value for τ_0 could be that of $PtRu_2$, this yields $k_{en} \sim 3.3 \times 10^5$ s^{-1}.

(50) Campagna, S.; Puntoriero, F.; Nastasi, F.; Bergamini, G.; Balzani, V. *Top. Curr. Chem.* **2007**, *280*, 117–214.